*Journal of Structural Chemistry. Vol. 56, No. 5, pp. 887-899, 2015.*


# MOLECULAR STRUCTURE AND VIBRATIONAL AND CHEMICAL SHIFT ASSIGNMENTS OF (4*R*)-5-ENO-4,7-EPIDIOXY-3,7-O-METHYL-1,2-O-(S)-TRICHLOROETHYLIDENE-5,6,8-TRIDEOXY-α-D-THREO-1,4-FURANO-4,7-DIULO-OCTOSE BY DFT AND *AB INITIO* HF CALCULATIONS

**T. Karakurt[1], M. Dinçer[2], and F. Çetin[3]**

UDC 548.737

Elemental analyses, single crystal X-ray diffraction method, and $^{1}H$ and $^{13}C$ NMR spectral techniques are used to synthesize and characterize the crystal structure of 4-diethylamino-2-{[4-(3-methyl-3-phenyl-cyclobutyl)-thiazol-2-yl]-hydrazonomethyl}-phenol. In order to calculate the molecular geometry along with vibrational frequencies and the gauge including atomic orbital (GIAO) $^{1}H$ and $^{13}C$ NMR chemical shift values of the title crystal structure in the ground state, the Hartree–Fock (HF) and density functional theory (DFT) methods with 6-311G(*d*,*p*) basis sets are utilized. The assignments of the vibrational frequencies are calculated with the help of the potential energy distribution (PED) analysis using the VEDA 4 software. Experimental data are used for comparison. The molecule contains C–H···O intra–inter–molecular interactions.

**DOI:** 10.1134/S0022476615050108

**Keywords:** X-ray structure determination, DFT, HF, GIAO, $^{1}H$ and $^{13}C$ NMR, IR spectra, vibrational assignment.

## INTRODUCTION

Malaria is a principal parasitic illness in many areas of South America, Asia, and Africa. While four types of malarial parasite infect humans, the majority of malaria cases are caused by *Plasmodium falciparum*, and its tenacity to many modern antimalarial drugs has entangled the problem of illness control [1]. Some of the actual combination therapies in clinical exercise for malaria cure rest up on endoperoxide-based compounds [2].

On the whole, the endoperoxides have some advantages over present antimalarial meds. First, there is cross-resistance with other antimalarial meds. Second, the endoperoxides clear the environmental blood of parasites more swiftly than other present meds do. Finally, resistance to the endoperoxides has not yet improved despite extensive clinical use [3]. Besides all these, there are some downsides. The endoperoxides have short half-lives, and effective levels in plasma are

[1]Department of Chemical Engineering, Faculty of Engineering and Architecture, Ahi Evran University, Kırşehir, Turkey; tuncaykarakurt@gmail.com. [2]Department of Physics, Faculty of Sciences, Ondokuz Mayıs University, Samsun, Turkey. [3]Department of Chemistry, Faculty of Arts and Sciences, Ege University, İzmir, Turkey. The text was submitted by the authors in English. *Zhurnal Strukturnoi Khimii*, Vol. 56, No. 5, pp. 945-957, September-October, 2015. Original article submitted February 12, 2014; revised July 31, 2014.

undamped for a just relatively curt revolution. As a result, a short period cure (less than 5 days) with the endoperoxides is generally integrated with an unacceptably high ratio (>10%) of recrudescent infections [4].

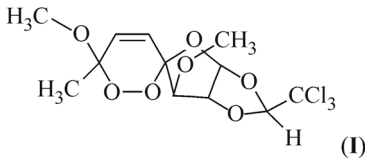
(**I**)

This paper reports the molecular and crystal structure of (4R)-5-eno-4,7-epidioxy-3,7-O-methyl-1,2-O-(S)-trichloroethylidene-5,6,8-trideoxy-α-D-threo-1,4-furano-4,7-diulo-octose ($C_{12}H_{15}Cl_3O_7$) (**I**) determined by the single crystal X-ray diffraction study.

Hartree–Fock (HF) and DFT (B3LYP) methods with the 6-311G(*d*,*p*) basis set were used in order to calculate the geometrical parameters, harmonic vibrational frequencies, and $^1$H and $^{13}$C NMR chemical shift values of the title crystal structure in the ground state. All ($C_{12}H_{15}Cl_3O_7$) parameters were calculated at the HF/6-311G(*d*,*p*) and B3LYP/6-311G(*d*,*p*) levels of theory with optimized geometries. These calculations are significant since they offer an insight into molecular parameters as well as IR and NMR spectra. The purpose of this study is to investigate the molecular and structural parameters of the chemical behavior of the title compound and to compare theoretical approximations with experimental investigations.

## COMPUTATIONAL DETAILS

Hartree–Fock (HF) and DFT(B3LYP) [5, 6] with the 6-311G(*d*,*p*) [7] basis set were utilized to optimize the molecular structure of the title crystal structure in the ground state (*in vacuo*). For modeling purposes, the initial prediction of the title crystal structure was taken from X-ray data. Following this, these methods were used to calculate the vibrational frequencies of the optimized molecular structures and scaled by 0.8929 and 0.9613 [8] respectively. $^1$H and $^{13}$C NMR spectra were calculated within the GIAO approach [9, 10] with the same methods and basis set as those utilized for the geometry optimization. The $^{13}$C and $^1$H NMR chemical shifts were converted to the TMS scale. This was reached by subtracting the calculated absolute chemical shielding of TMS ($\delta = \sum_0 - \sum$, where δ is the chemical shift, ∑ is the absolute shielding, and $\sum_0$ is the absolute shielding of TMS) with the following values, respectively: 32.60 ppm and 200.01 ppm for HF/6-311G(*d*,*p*) and 32.10 ppm and 189.40 ppm for B3LYP/6-311G(*d*,*p*). The calculations were carried out using the Gauss View Molecular Visualization [11, 12], the Gaussian 03 package [13], and the VEDA 4 program [14] for the crystal structure. The effects that the solvent had on theoretical NMR parameters were subsumed using the default model IEF–PCM [15] supplied by Gaussian 03. $CDCl_3$ with a dielectric constant (ϵ) of 4.81 was used as the solvent.

## EXPERIMENTAL

**Synthesis.** (4*R*)-5-eno-4,7-epidioxy-3-*O*-methyl-1,2-*O*-(*S*)-trichloroethylidene-5,6,8-trideoxy-α-D-*threo*-1,4-furano-4,7-diulo-octose (100 mg, 0.276 mmol) was dissolved in anhydrous methanol (25 ml). Dimethyl sulphite (2.58 ml, 0.552 mmol) was added to the solution and the reaction mixture was refluxed for 3 h. Solution was neutralized with diluted $NaHCO_3$, and the solvent was removed at 50°C. The syrupy residue was purified on a silica gel column, eluting with hexane-ethyl acetate (20:1).The solvent was removed to obtain the title product and it was crystallized from diethyl ether and light petroleum (Fig. 1). White crystals, yield 30% (0.32 mg), mp 147-148°C, $[\alpha]_D^{19}$ –99.0 (*c* 0.70, $CHCl_3$). IR (KBr, ν, $cm^{-1}$): 2963 (aliphatics), 1716 (–C=C–), 1361 (–C–H), 1156–1103 (–O–C–), 1038-983-811 (–O–O–), 619 (C–Cl). $^1$H NMR ($CDCl_3$, TMS, δ ppm): 1.45 (s, 3H,–$CH_3$), 3.43 (s, 3H,–$OCH_3$), 3.48 (s, 3H,–$OCH_3$), 3.72 (s, 1H, –H-3), 4.88 (d, 1H, H-2, $J_{H2,3}$ = 10.0 Hz), 5.73 (s, 1H, $HCCl_3$), 5.98 (d, 1H, H-5, $J_{H5,6}$ = 10.0 Hz), 6.06 (d, 1H, H-6, $J_{H5,6}$ = 10.0 Hz), 6.25 (d, 1H, H-1, $J_{H1,2}$ = 4.00 Hz). $^{13}$C NMR ($CDCl_3$, TMS, δ ppm): 134.3, 123.4, 112.7, 104.8, 104.3, 97.8, 95.6, 89.0, 87.2, 59.2, 59.4, 23.2.

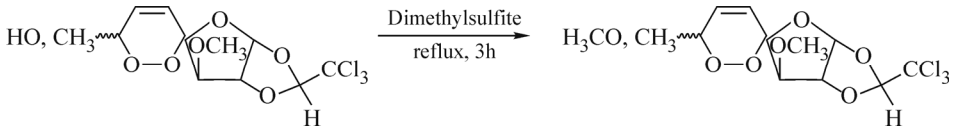


**Fig. 1.** Chemical structure of the title crystal structure.

The negative polarity APCI MS spectrum in methanol–choloroform produced ($M + Cl^-$) peaks at *m/z* 411, 413 (100%), 415, 417 (four chlorine isotope pattern), as the base peak group. Anal. Calcd. (%) for $C_{12}H_{15}Cl_3O_7$: C 38.30, H 3.98. Found: C 38.41, H 3.93.

**Crystallographic analysis.** All diffraction measurements were performed on the goniometer of a STOE diffractometer with an IPDS(II) image plate detector using graphite monochromated Mo$K_\alpha$ radiation ($\lambda = 0.71073$ Å) at room temperature (296 K). Data collections: Stoe X-AREA [16]. Cell refinement: Stoe X-AREA [16]. Data reduction: Stoe X-RED [18]. The structure was solved using direct methods with SHELXS-97 [19] and all non-hydrogen atoms were refined anisotropically by the full-matrix least squares procedure based on $F^2$ using SHELXL97 [17]. Molecular designs were acquired using ORTEP-III [18].

## RESULTS AND DISCUSSION

The title crystal structure, an ORTEP-III view of which can be seen in Fig. 2, crystallizes in the monoclinic space group $P2_1$ with two molecules in the unit cell. Additional information on the structure determinations is given in Table 1. The atomic numbering diagram for the title crystal structure ($C_{12}H_{15}Cl_3O_7$) and the theoretical geometric structure are shown in Fig. 2*a*, *b*.

The title molecule is built from planar fragments, *viz.* an endoperoxide ring *A*(C6/C8/C9/C10/O5/O6), a furan ring *B*(C3/C4/C6/C7/O4), and an acetal group. The endoperoxide ring forms a dihedral angle of 82.93(12)° with the furan ring. This dihedral angle was calculated as 80.40° at the HF/6-311G(*d*,*p*) level and as 80.60° at the B3LYP/6-311G(*d*,*p*) level. These experimental and theoretical results have shown that the title molecule is non-planar.

The molecule is stabilized by two intermolecular C2–H2···O3 and C11–H11A···O2, one intramolecular C12–H12C···O5, and one X–H···Cg (π-ring) intermolecular interactions (Fig. 3) whose characteristics are presented in Table 2. In the molecule, the C2 atom at (*x*, *y*, *z*) is doubled as a hydrogen-bond donor *via* the H2 atom to the O3 ring atom (–1+*x*, *y*, *z*), characterized by a C(10) motif, and the C11 atom at (*x*, *y*, *z*) acting as a hydrogen-bond donor via the H11A atom to the O2 ring atom at (–*x*, +*y*–1/2, –*z*+1/2) characterized by a C(10) motif [19], and the C12 carbon atom in the molecule acts as

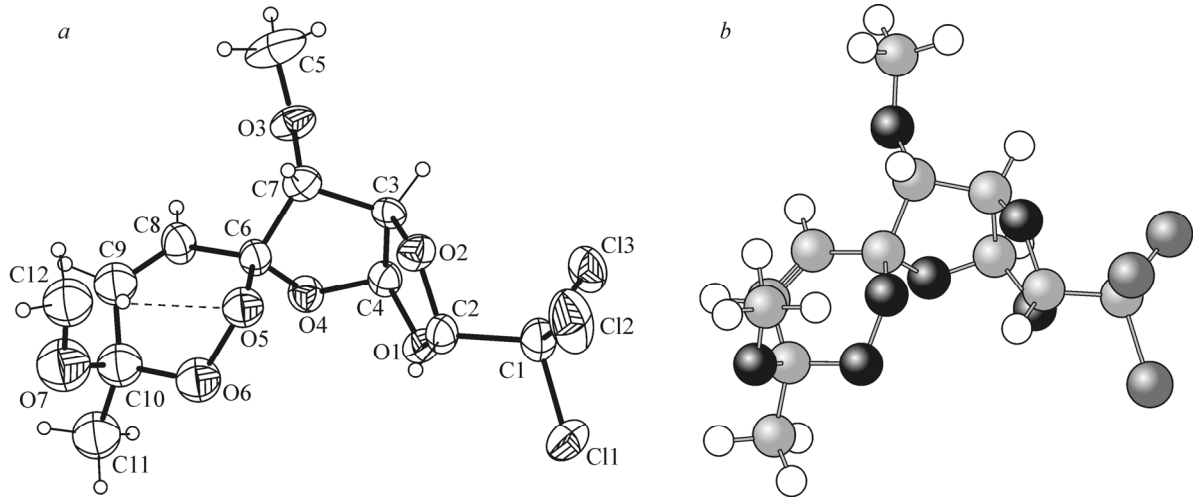


**Fig. 2.** Experimental geometric structure (*a*); theoretical geometric structure of the title crystal structure (*b*).

**TABLE 1.** Crystallographic Data for Title Crystal Structure

| | |
|---|---|
| Formula | $C_{12}H_{15}Cl_3O_7$ |
| Formula weight | 361.60 (a.k.b) |
| Temperature, K | 293 |
| Wavelength, Å | Mo$K_\alpha$, 0.71073 |
| Crystal system | Monoclinic |
| Space group | $P2_1$ |
| Unit cell: $a$, $b$, $c$, Å; β, deg | 6.5324(4), 11.2550(10), 11.4266(6); 103.759(4) |
| $V$, Å$^3$ | 816.00(9) |
| $Z$ | 2 |
| $D_{calc}$, g/cm$^3$ | 1.472 |
| $F$(000) | 388 |
| Crystal size, mm | 0.76×0.44×0.08 |
| $h$, $k$, $l$ range | $-8 \le h \le 8$, $-14 \le k \le 14$, $-14 \le l \le 14$ |
| Reflections collected | 16713 |
| Independent reflections | 3770 |
| Reflections observed [$I \ge 2\sigma(I)$] | 3126 |
| $R_{int}$ | 0.0468 |
| $R$ [$I > 2\sigma(I)$] | 0.0610 |
| $Rw$ [$I > 2\sigma(I)$] | 0.1801 |
| Goodness-of-fit on indicator | 1.044 |
| Structure determination | SHELXL97 (Sheldrick, 1997) |
| Extinction factor | 0.001(2) |
| $(\Delta\sigma)_{max}$, $(\Delta\sigma_{min})$, e/Å$^3$ | 0.790, –0.251 |

a hydrogen-bond donor *via* the H12C atom to the O5 ring atom in the molecule characterized by a S(6) motif [19] (Fig. 3). Crystal molecules are packed by normal van der Waals forces and π–π stacking interactions. The packing diagram of the title crystal structure is shown in the *bc* plane in Fig. 4, and the details of the hydrogen bond are presented in Table 2. The endoperoxide ring is planar with a maximum deviation of 0.006(3) Å for the C8 atom.

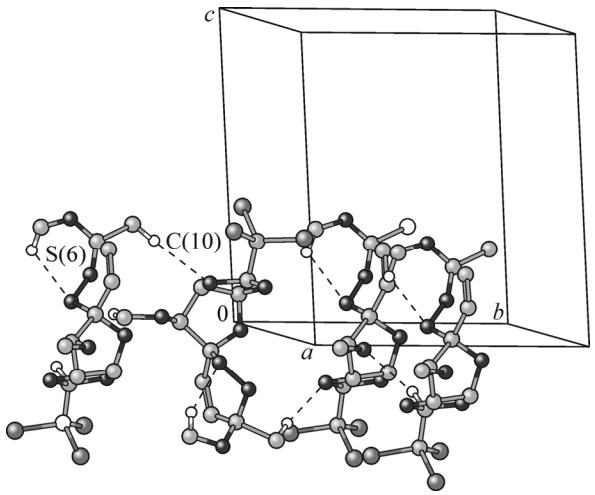


**Fig. 3.** Part of the crystal structure of the title crystal structure, showing C–H···O stacking interactions. For the sake of clarity, H atoms not involved in the motifs shown have been omitted.

**TABLE 2.** Hydrogen Bonding Geometry (Å, deg) for the Title Crystal Structure

| D–H…A | D–H | H…A | D…A | D–H…A |
|---|---|---|---|---|
| C2–H2…O3[i] | 1.01(2) | 2.45(2) | 3.44(2) | 165(12) |
| C11–H11A…O2[ii] | 0.96(2) | 2.57(3) | 3.53(3) | 173(3) |
| C12–H12C…O5 | 0.96(2) | 2.37(3) | 2.97(3) | 120(13) |

Symmetry code: [i] –1+*x*, *y*, *z*; [ii] 1–*x*, 1/2+*y*, *z*.

The dihedral angles between the endoperoxide plane, the furan plane, and the acetal group were as follows: 82.93(12)° (*AIB*) and 42.8(3)° (*AIC*). In light of all this, it can be argued that the compound is non-planar. These dihedral angles have been found to be 80.40° at the HF/6-311G(*d*,*p*) level and 80.60° at the B3LYP/6-311G(*d*,*p*) level. The theoretical and experimental results have shown that the title crystal structure is non-planar.

Different substituents depending on the endoperoxide ring are defined by the experimental bond lengths C8=C9 (1.30(7) Å), O6–C10 (1.42(6) Å), O5–C6 (1.43(5) Å), O5–O6 (1.44(5) Å). These bond lengths have been calculated as 1.33 Å, 1.45 Å, 1.42 Å, and 1.28 Å (for HF/6-311G(*d*,*p*)) respectively, and 1.31 Å, 1.41 Å, 1.39 Å, and 1.39 Å (for B3LYP/6-311G(*d*,*p*)) respectively. In the previous experimental work, the O–O and O–C bond lengths were found to be 1.47(13) Å and 1.41(15)-1.43(15) Å [20]. When the O5–C6–O4–C4–O1–C2–O2–C3 oxygen-carbon chain is considered, the bond distances commencing with C4–O1 are in sequence: short, long, short, long [21]. These distances are all within the ranges of a normal single bond or a partial double bond. It is possible that this pattern is caused by the delocalization of lone pairs on the oxygen atoms. If this is the case, it may has a stabilizing effect on the molecule. This is consistent with its high thermal stability. In the furan ring, the bond lengths of O4–C4 and C3–C4 were obtained to be 1.39(5) Å and 1.51(6) Å. These lengths were calculated as 1.41 Å and 1.54 Å using the HF/6-311G(*d*,*p*) method, and 1.38 Å and 1.53 Å using the B3LYP/6-311G(*d*,*p*) method, and the data are shown in Table 3 for the optimized geometric parameters. In our study, according to the HF and B3LYP methods, the optimized geometric parameters are much closer to the experimental data.

A rational method of a global comparison of the structures obtained by theoretical calculations is to superimpose the molecular framework with the one acquired from X-ray diffraction, which results in a RMSE of 0.172 Å for HF and 0.194 Å for B3LYP calculations (Fig. 5). Hence, the B3LYP method correlates better than the HF one for the calculated values.

**Assignments of the vibrational modes.** A Mattson 1000 Fourier transform (FT)-IR spectrophotometer with KBr pellets was used to measure IR spectra. To be able to reach the spectroscopic signing of the compounds, a frequency

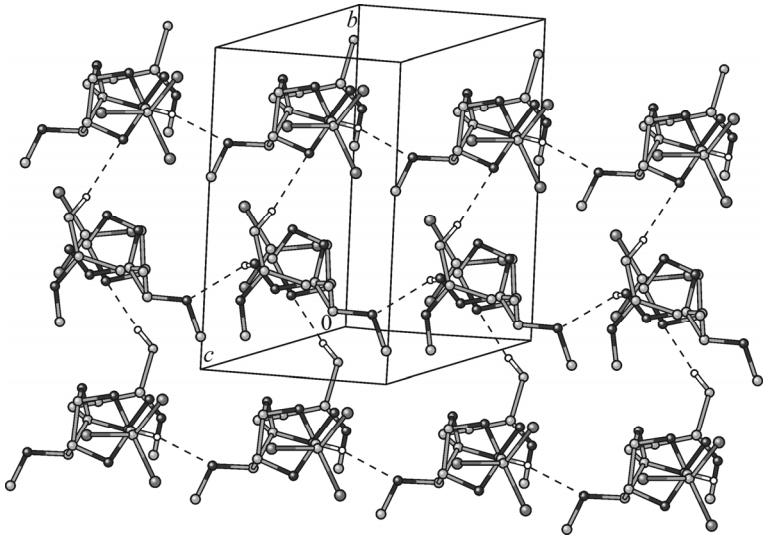


**Fig. 4.** Crystal packing of the title crystal structure projected on the *bc* plane. The dashed lines indicate the intermolecular hydrogen bonds.

**TABLE 3.** Selected Optimized and Experimental Geometric Parameters in the Ground State

| Bond lengths, Å | Experimental | HF | DFT | Bond lengths, Å | Experimental | HF | DFT |
|---|---|---|---|---|---|---|---|
| C2–C1 | 1.54(5) | 1.55 | 1.54 | O5–O6 | 1.44(5) | 1.28 | 1.39 |
| C4–O1 | 1.42(5) | 1.42 | 1.38 | C10–O6 | 1.41(6) | 1.45 | 1.41 |
| C4–C3 | 1.52(6) | 1.54 | 1.53 | C9–C8 | 1.30(7) | 1.33 | 1.31 |
| C3–O2 | 1.43(4) | 1.42 | 1.40 | C9–C10 | 1.48(8) | 1.50 | 1.51 |
| C5–O3 | 1.36(7) | 1.42 | 1.40 | C8–C6 | 1.50(5) | 1.49 | 1.49 |
| O4–C4 | 1.39(5) | 1.41 | 1.38 | C10–O7 | 1.29(10) | 1.41 | 1.38 |
| O5–C6 | 1.43(5) | 1.42 | 1.39 | C1–Cl1 | 1.75(4) | 1.76 | 1.76 |
| O3–C7 | 1.40(4) | 1.41 | 1.39 | RMS | | 0.0632 | 0.0476 |
| Bond angles, deg | Experimental | HF | DFT | Torsion angles, deg | Experimental | HF | DFT |
| Cl2–C1–Cl1 | 108.72(3) | 109.39 | 109.86 | O1–C2–C1–Cl1 | 60.12(6) | 59.39 | 59.45 |
| O1–C2–C1 | 109.33(4) | 110.36 | 109.52 | C4–O1–C2–C1 | –118.42(4) | –130.37 | –134.54 |
| O2–C2–O1 | 109.23(3) | 107.23 | 107.88 | C3–O2–C2–O1 | –8.50(4) | 4.31 | 7.75 |
| C4–C3–C7 | 104.55(4) | 105.37 | 104.06 | C5–O3–C7–C6 | 132.98(7) | 159.30 | 161.21 |
| O3–C7–C6 | 108.94(4) | 108.57 | 108.35 | C5–O3–C7–C3 | –116.56(7) | –90.05 | –87.51 |
| O4–C4–C3 | 108.59(3) | 109.08 | 106.87 | C10–O6–O5–C6 | –69.27(6) | –73.69 | –72.18 |
| C5–O3–C7 | 115.88(5) | 113.13 | 115.35 | | | | |
| O7–C10–C11 | 106.88(5) | 106.72 | 105.99 | | | | |
| C9–C8–C6 | 119.33(4) | 119.37 | 119.31 | | | | |
| RMS | | 1.2761 | 0.9453 | | | | |

calculation assay was made. The harmonic vibrational frequencies were calculated for the crystal structures with the help of HF/6-311G(*d*,*p*) and B3LYP/6-311G(*d*,*p*) methods, and detailed PED assignments are shown in Table 4. The experimental and calculated frequencies and IR intensities of the structure can be seen in Table 4. The table also lists the harmonic vibrational frequencies in the range region 4000-400 $cm^{-1}$. Any variety between the calculated and observed frequencies can be attributed to two facts: that the experimental results appertain to the solid phase while theoretical calculations appertain to the gaseous one; and that the calculations were actually made on a single molecule while experimental values were obtained in relation to intermolecular interactions.

The 105 normal vibrational modes of the title crystal structure composed of 37 atoms, spanning in irreducible renditions as 105A under the C1 point group symmetry, were designated based on the motion of singular atoms. The calculated IR intensity (Rel. intensity) enables the identification of the strength of the transition. It should be remembered that experimental IR spectra are often reported in either percent transmission or absorbance units. Fig. 6 displays the simulated IR spectra where the intensity is plotted against the harmonic vibrational frequencies and also the experimental IR spectra.

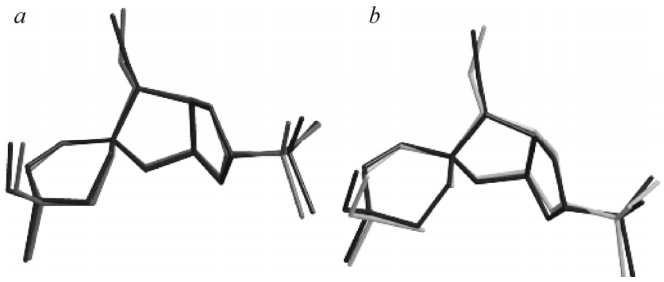


**Fig. 5.** Atom-by-atom superimposition of the calculated structures (*a* = HF; *b* = B3LYP with 6-311G(*d*,*p*)) over the X-ray structure (black) for the title crystal structure. Hydrogen atoms are omitted for clarity.

**TABLE 4.** Comparison of the Experimental and Calculated Vibrational Spectra of the Title Crystal Structure

| Mode Nos. | Experimental FT-IR, $cm^{-1}$ | HF/6-311G(*d*,*p*) | | | B3LYP/6-311G(*d*,*p*) | | | Assigments with PED, % (≥10%) |
|---|---|---|---|---|---|---|---|---|
| | | Unscaled | Scaled | $I_{IR}$ | Unscaled | Scaled | $I_{IR}$ | |
| 1 | 2 | 3 | 4 | 5 | 6 | 7 | 8 | 9 |
| 1 | – | 3428 | 3061 | 0 | 3240 | 3115 | 0 | $\nu_{CH}(98)$ |
| 2 | – | 3374 | 3012 | 0 | 3193 | 3069 | 0 | $\nu_{CH}(96)$ |
| 3 | – | 3361 | 3001 | 1 | 3170 | 3047 | 0 | $\nu_{CH}(94)$ |
| 4 | – | 3324 | 2968 | 1 | 3157 | 3035 | 1 | $\nu_{CH}(98)$ |
| 5 | – | 3320 | 2965 | 0 | 3156 | 3033 | 0 | $\nu_{CH}(96)$ |
| 6 | – | 3320 | 2964 | 1 | 3153 | 3031 | 1 | $\nu_{CH}(92)$ |
| 7 | 2963 | 3319 | 2963 | 1 | 3145 | 3023 | 0 | $\nu_{CH}(97)$, asym, $CH_3$ |
| 8 | – | 3313 | 2958 | 2 | 3112 | 2992 | 1 | $\nu_{CH}(97)$ |
| 9 | – | 3312 | 2957 | 6 | 3111 | 2990 | 6 | $\nu_{CH}(92)$ |
| 10 | – | 3297 | 2944 | 1 | 3087 | 2967 | 1 | $\nu_{CH}(100)$ |
| 11 | – | 3282 | 2931 | 0 | 3081 | 2961 | 0 | $\nu_{CH}(97)$ |
| 12 | – | 3256 | 2908 | 1 | 3078 | 2959 | 0 | $\nu_{CH}(96)$ |
| 13 | – | 3235 | 2888 | 1 | 3067 | 2949 | 1 | $\nu_{CH}(97)$ |
| 14 | – | 3224 | 2879 | 1 | 3041 | 2923 | 1 | $\nu_{CH}(14)+\nu_{CH}(81)$ |
| 15 | – | 3200 | 2857 | 2 | 3015 | 2898 | 1 | $\nu_{CH}(92)$ |
| 16 | 1716 | 1902 | 1698 | 1 | 1738 | 1671 | 0 | $\nu_{CC}(65)$ |
| 17 | – | 1662 | 1484 | 3 | 1538 | 1478 | 1 | $\delta_{HCH}(66)$ |
| 18 | – | 1660 | 1482 | 2 | 1537 | 1477 | 3 | $\delta_{HCH}(71)+\tau_{HCOC}(15)$ |
| 19 | – | 1650 | 1473 | 3 | 1522 | 1463 | 1 | $\tau_{HCOC}(15)$ |
| 20 | – | 1647 | 1471 | 4 | 1519 | 1460 | 3 | $\delta_{HCH}(69)+\tau_{HCOC}(23)$ |
| 21 | – | 1639 | 1464 | 1 | 1517 | 1458 | 1 | $\delta_{HCH}(68)+\tau_{HCCC}(22)$ |
| 22 | – | 1636 | 1461 | 5 | 1511 | 1453 | 5 | $\tau_{HCCC}(21)+\delta_{HCH}(71)$ |
| 23 | – | 1631 | 1456 | 2 | 1504 | 1446 | 2 | $\delta_{HCH}(79)$ |
| 24 | – | 1629 | 1454 | 2 | 1500 | 1442 | 2 | $\delta_{HCH}(86)$ |
| 25 | – | 1566 | 1398 | 5 | 1431 | 1375 | 4 | $\delta_{HCC}(83)$ |
| 26 | – | 1565 | 1397 | 7 | 1423 | 1368 | 4 | – |
| 27 | – | 1564 | 1396 | 6 | 1417 | 1362 | 4 | $\delta_{HCO}(51)+\delta_{HCOC}(14)$ |
| 28 | – | 1555 | 1388 | 10 | 1402 | 1348 | 8 | $\delta_{HCO}(44)+\delta_{HCO}(18)$ |
| 29 | – | 1540 | 1375 | 4 | 1387 | 1334 | 4 | $\delta_{HCO}(16)+\delta_{HCO}(24)+\tau_{HCOC}(36)$ |
| 30 | 1361 | 1523 | 1360 | 3 | 1372 | 1319 | 3 | $\tau_{HCOC}(27)+\delta_{HCO}(33)$ |
| 31 | – | 1508 | 1347 | 3 | 1353 | 1301 | 3 | $\delta_{HCO}(17)+\delta_{HCO}(11)+\tau_{HCOC}(35)$ |
| 32 | – | 1457 | 1301 | 11 | 1327 | 1275 | 10 | $\tau_{HCOC}(34)+\delta_{HCO}(21)+\delta_{HCO}(15)$ |
| 33 | – | 1455 | 1299 | 4 | 1319 | 1268 | 6 | $\delta_{HCO}(53)$ |
| 34 | – | 1435 | 1281 | 5 | 1287 | 1237 | 6 | $\nu_{CC}(13)+\tau_{HCOC}(11)$ |
| 35 | – | 1400 | 1250 | 4 | 1267 | 1218 | 96 | $\tau_{HCOC}(20)$ |
| 36 | – | 1380 | 1232 | 107 | 1250 | 1202 | 10 | $\tau_{HCOC}(18)+\delta_{HCC}(19)$ |
| 37 | – | 1366 | 1219 | 10 | 1232 | 1184 | 21 | $\tau_{HCOC}(39)$ |
| 38 | – | 1355 | 1210 | 2 | 1213 | 1166 | 2 | – |
| 39 | – | 1352 | 1207 | 7 | 1201 | 1155 | 10 | $\tau_{HCOC}(29)+\nu_{CC}(11)$ |
| 40 | – | 1332 | 1189 | 18 | 1196 | 1150 | 6 | $\tau_{HCOC}(27)$ |
| 41 | – | 1312 | 1172 | 138 | 1192 | 1146 | 192 | $\delta_{HCH}(16)+\tau_{HCOC}(49)$ |
| 42 | – | 1305 | 1166 | 69 | 1187 | 1141 | 102 | $\tau_{HCOC}(23)+\nu_{OC}(12)$ |

**TABLE 4.** (Cont.)

| 1 | 2 | 3 | 4 | 5 | 6 | 7 | 8 | 9 |
|---|---|---|---|---|---|---|---|---|
| 43 | – | 1298 | 1159 | 72 | 1181 | 1135 | 38 | $\tau_{HCOC}(10)+\tau_{HCOC}(28)+$ $+\nu_{OC}(10)+\delta_{HCH}(12)$ |
| 44 | 1156 | 1295 | 1156 | 29 | 1164 | 1119 | 15 | $\nu_{OC}(19)+\nu_{OC}(15)$ |
| 45 | 1103 | 1271 | 1135 | 22 | 1148 | 1103 | 14 | $\nu_{OC}(13)+\nu_{OC}(20)+\tau_{HCCC}(16)$ |
| 46 | – | 1266 | 1130 | 12 | 1128 | 1085 | 6 | $\nu_{OC}(21)$ |
| 47 | – | 1238 | 1106 | 32 | 1102 | 1059 | 22 | $\nu_{OC}(12)+\nu_{OC}(41)$ |
| 48 | – | 1221 | 1090 | 15 | 1088 | 1046 | 41 | $\nu_{OC}(11)$ |
| 49 | – | 1216 | 1086 | 41 | 1071 | 1030 | 4 | $\nu_{CC}(45)$ |
| 50 | 1038 | 1209 | 1080 | 26 | 1048 | 1008 | 142 | $\nu_{OC}(32)+\nu_{OO}(45)$ |
| 51 | – | 1188 | 1060 | 10 | 1043 | 1002 | 26 | $\nu_{CC}(35)$ |
| 52 | – | 1154 | 1030 | 17 | 1028 | 988 | 6 | $\nu_{OC}(10)+\nu_{OC}(14)$ |
| 53 | – | 1152 | 1029 | 52 | 1012 | 972 | 226 | $\nu_{OC}(37)$ |
| 54 | 1013 | 1135 | 1013 | 9 | 1000 | 962 | 22 | $\tau_{HCCC}(77)$ |
| 55 | – | 1131 | 1010 | 78 | 998 | 960 | 5 | $\nu_{OC}(12)+\nu_{OC}(10)+\nu_{OC}(13)+$ $+\nu_{CC}(22)+\gamma_{COOC}(11)+$ |
| 56 | 983 | 1106 | 987 | 88 | 987 | 948 | 127 | $\nu_{OO}(24)\nu_{OC}(10)+\nu_{OC}(14)$ |
| 57 | 950 | 1095 | 978 | 196 | 940 | 903 | 30 | $\nu_{OC}(17)+\tau_{HCCC}(20)+\nu_{OO}(15)$ |
| 58 | – | 1026 | 917 | 72 | 916 | 881 | 38 | $\nu_{OC}(26)+\tau_{HCCC}(10)$ |
| 59 | – | 1006 | 898 | 60 | 905 | 870 | 60 | $\tau_{COCO}(12)+\delta_{COC}(19)$ |
| 60 | – | 995 | 889 | 267 | 892 | 858 | 200 | $\tau_{HCOC}(12)+\gamma_{CCOC}(10)$ |
| 61 | 888 | 982 | 877 | 170 | 880 | 846 | 166 | $\nu_{OO}(50)$ |
| 62 | 853 | 965 | 861 | 8 | 860 | 827 | 37 | $\nu_{OC}(20)+\delta_{COC}(11)$ |
| 63 | – | 946 | 844 | 9 | 845 | 812 | 116 | $\delta_{COC}(17)$ |
| 64 | – | 937 | 837 | 82 | 820 | 788 | 218 | $\gamma_{ClCCCl}(12)+\gamma_{COOC}(16)+$ $+\nu_{OC}(13)+\nu_{ClC}(20)+$ |
| 65 | 811 | 926 | 826 | 81 | 790 | 760 | 107 | $\delta_{CCO}(12)+\nu_{OO}(13)+\gamma_{ClCCCl}(12)+$ $+\nu_{ClC}(55)+\delta_{CCO}(12)$ |
| 66 | 756 | 869 | 776 | 143 | 777 | 747 | 69 | $\tau_{HCCC}(77)$ |
| 67 | 748 | 840 | 750 | 268 | 755 | 726 | 77 | $\nu_{OC}(21)+\nu_{ClC}(11)+\delta_{OCO}(46)$ |
| 68 | – | 820 | 733 | 369 | 745 | 716 | 9 | $\nu_{OC}(14)+\delta_{CCO}(20)+\delta_{CCC}(17)$ |
| 69 | – | 726 | 648 | 16 | 657 | 632 | 25 | $\delta_{COO}(14)+\delta_{COC}(15)$ |
| 70 | – | 703 | 627 | 45 | 638 | 613 | 8 | $\nu_{CC}(31)$ |
| 71 | 619 | 695 | 621 | 77 | 623 | 599 | 34 | $\nu_{ClC}(44)+\gamma_{COOC}(21)$ |
| 72 | – | 669 | 597 | 5 | 611 | 588 | 10 | $\delta_{COC}(18)+\nu_{CC}(21)$ |
| 73 | – | 649 | 579 | 10 | 589 | 566 | 7 | $\delta_{OCO}(13)+\delta_{COO}(39)$ |
| 74 | – | 617 | 551 | 18 | 558 | 536 | 5 | $\delta_{OCO}(15)+\delta_{CCC}(11)$ |
| 75 | – | 575 | 513 | 6 | 523 | 503 | 5 | $\delta_{OCO}(35)$ |
| 76 | – | 543 | 485 | 22 | 490 | 471 | 5 | $\delta_{OCO}(18)+\tau_{CCCO}(11)$ |
| 77 | – | 528 | 471 | 51 | 481 | 462 | 25 | $\delta_{CCO}(10)$ |
| 78 | – | 498 | 445 | 27 | 456 | 438 | 16 | $\delta_{CCO}(10)$ |
| 79 | – | 452 | 403 | 24 | 413 | 397 | 2 | $\nu_{ClC}(18)$ |
| 80 | – | 426 | 381 | 15 | 389 | 374 | 23 | $\nu_{ClC}(26)$ |
| 81 | – | 415 | 370 | 15 | 381 | 366 | 11 | $\delta_{CCO}(18)+\gamma_{CCOC}(15)$ |
| 82 | – | 391 | 350 | 0 | 353 | 340 | 1 | $\delta_{CCO}(16)+ \nu_{ClC}(25)$ |
| 83 | – | 365 | 326 | 2 | 337 | 324 | 2 | $\delta_{COC}(14)+ \delta_{COC}(17)$ |

**TABLE 4.** (Concl.)

| 1 | 2 | 3 | 4 | 5 | 6 | 7 | 8 | 9 |
|---|---|---|---|---|---|---|---|---|
| 84 | – | 334 | 298 | 2 | 303 | 292 | 2 | |
| 85 | – | 321 | 287 | 1 | 292 | 281 | 1 | $\delta_{ClCCl}(11)+\delta_{ClCCl}(12)+$ $+\gamma_{ClCClC}(31)+\nu_{ClC}(15)$ |
| 86 | – | 319 | 285 | 4 | 289 | 277 | 4 | $\gamma_{ClCClC}(18)$ |
| 87 | – | 300 | 268 | 3 | 275 | 265 | 5 | $\delta_{OCC}(12)+\delta_{COC}(11)+$ $+\delta_{COC}(13)+\tau_{HCOC}(12)$ |
| 88 | – | 269 | 240 | 10 | 244 | 234 | 12 | $\tau_{HCOC}(13)+\tau_{COOC}(13)$ |
| 89 | – | 261 | 233 | 7 | 236 | 227 | 9 | $\delta_{ClCCl}(11)+\delta_{ClCCl}(20)$ |
| 90 | – | 259 | 231 | 4 | 227 | 218 | 3 | $\tau_{HCCC}(87)$ |
| 91 | – | 232 | 207 | 51 | 220 | 212 | 52 | $\tau_{HCOC}(77)$ |
| 92 | – | 225 | 201 | 40 | 204 | 196 | 36 | $\gamma_{ClCClC}(10)+\delta_{ClCCl}(46)$ |
| 93 | – | 220 | 196 | 14 | 199 | 191 | 49 | $\delta_{ClCCl}(12)+\delta_{ClCCl}(10)+\delta_{ClCCl}(10)$ |
| 94 | – | 199 | 178 | 56 | 183 | 176 | 8 | $\tau_{HCOC}(11)+\tau_{CCCO}(16)+\gamma_{ClCClC}(10)$ |
| 95 | – | 183 | 164 | 13 | 166 | 160 | 10 | $\gamma_{COOC}(12)+\delta_{ClCCl}(22)$ |
| 96 | – | 167 | 149 | 50 | 160 | 154 | 18 | $\delta_{OCC}(18)+\tau_{HCOC}(45)$ |
| 97 | – | 133 | 119 | 16 | 127 | 122 | 32 | – |
| 98 | – | 120 | 107 | 29 | 107 | 103 | 22 | $\tau_{COCO}(55)$ |
| 99 | – | 105 | 94 | 15 | 98 | 94 | 36 | – |
| 100 | – | 92 | 82 | 37 | 88 | 85 | 23 | $\tau_{COCC}(49)$ |
| 101 | – | 80 | 71 | 28 | 75 | 72 | 9 | $\tau_{CCCO}(35)$ |
| 102 | – | 64 | 58 | 33 | 59 | 57 | 24 | $\tau_{COCO}(11)+\gamma_{OCOC}(12)+\delta_{COC}(12)$ |
| 103 | – | 53 | 47 | 31 | 48 | 46 | 10 | – |
| 104 | – | 30 | 27 | 9 | 27 | 26 | 8 | – |
| 105 | – | 27 | 24 | 2 | 22 | 22 | 3 | $\tau_{COCO}(60)$ |

ν: stretching, δ: in-plane bending, γ: out-of-plane bending, τ: torsion, asym: asymmetric stretching; $I_{IR}$: IR intensity ($K \cdot mmol^{-1}$).

The C–H stretching vibration of the methoxy group band observed in the FT-IR spectrum at 2963 $cm^{-1}$ is assigned to $CH_3$ asymmetric stretching vibrations. The theoretical values scaled by the B3LYP/6-311G(*d*,*p*) method at 3023 $cm^{-1}$ are also in good accordance with the experimental values. The O–$CH_3$ vibrational mode at ~40 $cm^{-1}$ is assigned to anisole [22] and in the range 100-1000 $cm^{-1}$ to anisole and its derivatives [23-26]. This mode at 1026 $cm^{-1}$, 909 $cm^{-1}$, and 995 $cm^{-1}$ is assigned to *o*-, *m*-, and *p*-methoxy benzaldehydes respectively. In our study, the O–$CH_3$ stretching mode is observed at 1038 $cm^{-1}$. The theoretically computed value is found at 1080 $cm^{-1}$ (HF/6-311G(*d*,*p*)) and 1008 $cm^{-1}$ (B3LYP/6-311G(*d*,*p*)). The C–O–$CH_3$ angle bending mode was designated close to 300 $cm^{-1}$ by Owen and Hester [27] and at 421 $cm^{-1}$ by Campagnaro and Wood [28]. Rao et al. [29-32] have recommended an assignment for this mode in the range 300-670 $cm^{-1}$. Singh and Yadav [33] assigned the C–O–$CH_3$ angle bending mode at 341 $cm^{-1}$, 382 $cm^{-1}$, and 430 $cm^{-1}$ to *o*-, *m*-, and *p*-methoxy benzaldehydes respectively. By the B3LYP/6-311G(*d*,*p*) method we have calculated the C–O–$CH_3$ angle bending mode to be at 324 $cm^{-1}$.

The asymmetric C–O–C stretching vibration produces a strong band at 1261 $cm^{-1}$ in the IR spectrum [34, 35]. The symmetric C–O–C stretching vibration looks like a weak band at 1076 $cm^{-1}$ in the IR spectrum [34, 35]. Fukukawa and Ueda [36] reported the symmetric C–O–C stretch at 1045 $cm^{-1}$ for benzoxazole. In our study, the DFT calculation gives 1046 $cm^{-1}$ for the symmetric C–O–C mode, 1119 $cm^{-1}$ for asymmetric C–O–C modes of the title crystal structure. The asymmetric and symmetric C–O–C modes of the title crystal structure are listed in Table 4. Every refracting of the calculated wavenumber for this mode can be ascribed to the underestimation of a high degree of π-electron delocalization based on the formation of hydrogen bonds or conjugation [37].

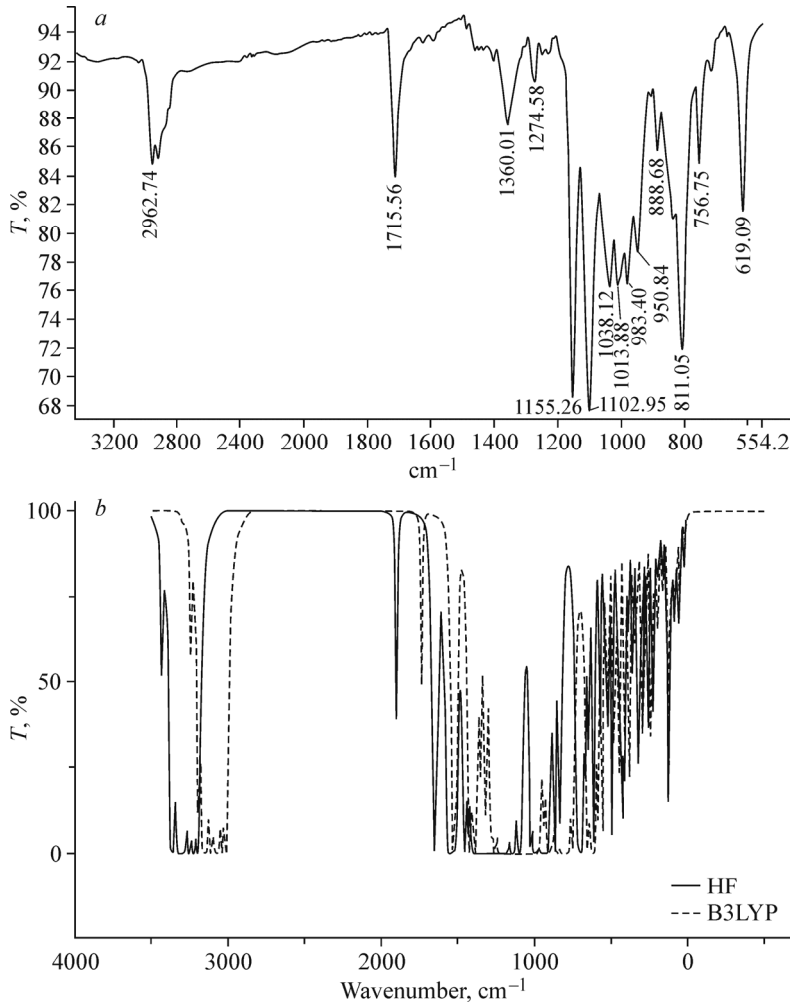


**Fig. 6.** FT-IR spectrum of the title crystal structure (*a*), simulated (HF and B3LYP levels) IR spectra of the title crystal structure (*b*).

Vibrational modes of methoxy groups are known to be due to a diversity of interesting interactions, for instance, electronic effects, Fermi resonance, and intermolecular hydrogen bonding [38]. Electronic effects mostly caused by the presence of the oxygen atom adjacent to the $CH_3$ group can recast the position of C–H stretching and bending modes [39-41].

The aromatic C–H in-plane bending vibration is observed in the range 1300-1000 $cm^{-1}$. Although the bands are strong, they have a weak to medium intensity [42]. This shows great accordance with the theoretically scaled frequency values at 1347 $cm^{-1}$ (HF/6-311G(*d*,*p*)) and at 1301 $cm^{-1}$ (B3LYP/6-311G(*d*,*p*)).

Table 4 presents the theoretical and experimental results for the title crystal structure. The vibrational frequencies were obtained using the Gauss–View software.

**Assignments of the chemical shift values.** The $^1H$ NMR and $^{13}C$ NMR spectra were recorded on a Varian Mercury spectrometer using tetramethylsilane (TMS) as the internal reference (Fig. 7*a* and *b*). GIAO $^1H$ and $^{13}C$ chemical shift calculations were made using the HF and B3LYP methods with the 6-311G(*d*,*p*) basis set for the optimized geometry. The results are listed in Table 5. We included the average values for the $CH_3$ group of the experimental $^1H$ chemical shift values. Due to deshielding by the electronegative property of the O atom, the chemical shift values of C6 and C2 are greater than the others and are observed at 134.3 ppm and 123.4 ppm, which is consistent with the values reported previously (104.7 ppm and 114.7 ppm, [43]). Similarly, endoperoxide carbon peaks are observed at 112.7 ppm and 97.8 ppm. In addition, the chemical shift values of C5, C11, and C12 atoms are lower than the other carbon peaks because of the shielding effect that is the non-electronegative characteristic of the hydrogen atom. It is important to mention that the electron emitting atom or group

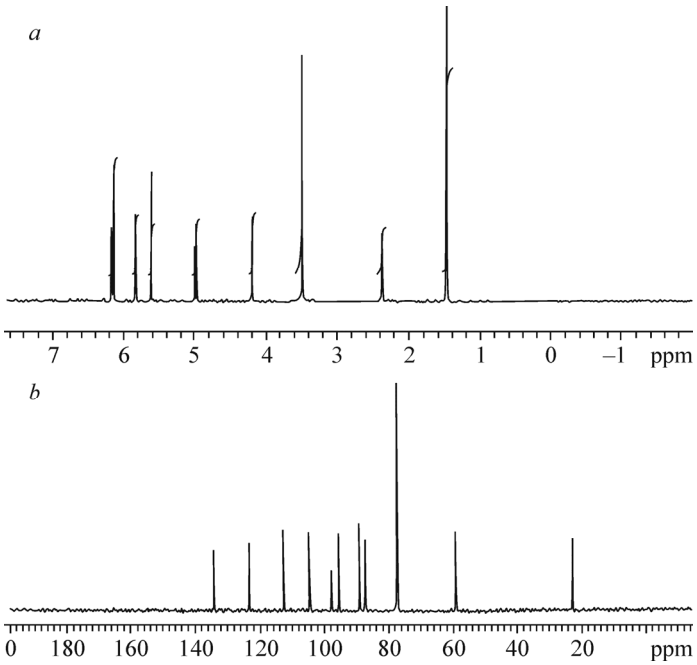


**Fig. 7.** $^{1}$H NMR spectrum (*a*); $^{13}$C NMR spectrum of the title crystal structure (*b*).

enhances the shielding and moves the resonance to lower frequencies. Conversely, the electronegative atom or the nearby electron-withdrawing atom or group can reduce the shielding, and move the resonance of the attached proton to higher frequencies. The chemical shifts obtained and computed for the hydrogen atoms of methyl groups are rather low. All values are ≤ 3 ppm [44] due to the shielding effect. The data of this study show that the methyl protons at C5/C11/C12 appear as a singlet with a three-proton integral at 1.45 ppm and is in good agreement with the computed chemical shift values shown in Table 5. In order to compare the theoretical and experimental data, we studied the relativity between the calculation and the experiments and concluded that the linear function formula is $y = 0.934x - 0.32$ for HF; where $R^2$ is 0.9940, $y = 1.202x + 0.2631$ for B3LYP; where $R^2$ is 0.9981. The results suggest that the B3LYP method has better fit with the experimental values than HF in evaluating the $^{1}$H and $^{13}$C chemical shifts.

**TABLE 5.** Theoretical and Experimental $^{13}$C and $^{1}$H Isotropic Chemical Shifts (with respect to TMS, all values in ppm)

| Atom | Experimental, ppm ($CDCl_3$) | HF | DFT | Atom | Experimental, ppm ($CDCl_3$) | HF | DFT |
|---|---|---|---|---|---|---|---|
| C1 | 104.3 | 100.40 | 98.84 | H(C2–H) | 5.73 | 5.28 | 5.72 |
| C2 | 123.4 | 93.02 | 122.4 | H(Methyl) | 1.45 | 1.1-3.56 | 1.3-2.99 |
| C3 | 104.8 | 68.81 | 102.14 | H(C4–H) | 6.25 | 5.7 | 6.19 |
| C4 | 87.20 | 91.31 | 90.62 | H(C3–H) | 4.80 | 4.33 | 4.32 |
| C5 | 59.20 | 45.40 | 52.11 | H(C7–H) | 3.72 | 3.21 | 3.45 |
| C6 | 134.3 | 127.29 | 95.88 | H(C8–H) | 6.10 | 6.09 | 6.85 |
| C7 | 89.10 | 73.67 | 76.12 | H(C9–H) | 6.2 | 6.4 | 6.1 |
| C8 | 112.7 | 124.64 | 121.55 | | | | |
| C9 | 97.80 | 92.79 | 131.5 | | | | |
| C10 | 95.6 | 86.79 | 91.33 | | | | |
| C11 | 23.2 | 20.12 | 21.55 | | | | |
| C12 | 47.4 | 41.53 | 44.55 | | | | |

## CONCLUSIONS

The current study computed, compared, and reported the experimental geometric parameters, vibrational frequencies, and chemical shifts of the title crystal structure in an attempt to test the HF and DFT levels. The B3LYP level of theory including the electron correlation effects is found to have better fit with the experimental geometric parameters, chemical shifts, and vibrational frequencies than the HF method. We hope this article will be useful in the design and synthesis of new materials.

CCDC-889093 contains the supplementary crystallographic data for the compound reported in this paper. These data can be obtained free of charge at www.ccdc.cam.ac.uk/conts/retrieving.html (or from the Cambridge Crystallographic Data Centre (CCDC), 12 Union Road, Cambridge CB2 1EZ, UK; fax: +44(0)1223-336033; e-mail: deposit@ccdc.cam.ac.uk).

The Research Centre of the Ondokuz Mayıs University (Project No: F-461) is acknowledged for the support. In addition, computing resources used in this work were provided by the National Center for High Performance Computing of Turkey (UHeM) under grant number 1002742013, and the financial support of this work by the Ahi Evran University Scientific Research Fund under contract no. PYO-FEN.4001.13.011 is gratefully acknowledged.

## REFERENCES

1. J. P. J. Daily, *Clin. Pharmacol*., **46**, 1487 (2006).
2. S. R. Meshnick, T. E. Taylor, and S. Kamchonwongpaisan, *Microbiol. Rev*., **60,** 301 (1996).
3. N. J. White, *Trans. R. Soc. Trop. Med. Hyg*., **88**, S3/S4 (1994).
4. C. Lee, W. Yang, and R. G Parr, *Phys. Rev*., **B37**, 785-789 (1988).
5. A. D. Becke, *J. Chem. Phys*., **98**, 5648-5652 (1993).
6. R. Ditchfield, W. J. Hehre, and J. A. Pople, *J. Chem. Phys*., **54**, 724-728 (1971).
7. J. B. Foresman and A. Frisch, *Exploring Chemistry with Electronic Structure Methods*, 2nd ed., Gaussian Inc., Pittsburgh (1996).
8. R. Ditchfield, *J. Chem. Phys*., **56**, 5688-5691 (1972).
9. K. Wolinski, J. F. Hinton, and P. Pulay, *J. Am. Chem. Soc*., **112**, 8251-8260 (1990).
10. R. Dennington II, T. Keith, and J. Millam, *GaussView, Version 4.1.2,* Semichem Inc., Shawnee Mission, KS (2007).
11. A. Frisch, R. Dennington II, T. Keith, J. Millam, A. B. Nielsen, A. J. Holder, and J. Hiscocks, *GaussView Reference, Version 4.0*, Gaussian Inc., Pittsburgh (2007).
12. M. J. Frisch, G. W. Trucks, H. B. Schlegel, G. E. Scuseria, M. A. Robb, J. R. Cheeseman, J. A. Montgomery Jr., T. Vreven, K. N. Kudin, J. C. Burant, J. M. Millam, S. S. Iyengar, J. Tomasi, V. Barone, B. Mennucci, M. Cossi, G. Scalmani, N. Rega, G. A. Petersson, H. Nakatsuji, M. Hada, M. Ehara, K. Toyota, R. Fukuda, J. Hasegawa, M. Ishida, T. Nakajima, Y. Honda, O. Kitao, H. Nakai, M. Klene, X. Li, J. E. Knox, H. P. Hratchian, J. B. Cross, V. Bakken, C. Adamo, J. Jaramillo, R. Gomperts, R. E. Stratmann, O. Yazyev, A. J. Austin, R. Cammi, C. Pomelli, J. W. Ochterski, P. Y. Ayala, K. Morokuma, G. A. Voth, P. Salvador, J. J. Dannenberg, V. G. Zakrzewski, S. Dapprich, A. D. Daniels, M. C. Strain, O. Farkas, D. K. Malick, A. D. Rabuck, K. Raghavachari, J. B. Foresman, J. V. Ortiz, Q. Cui, A. G. Baboul, S. Clifford, J. Cioslowski, B. B. Stefanov, G. Liu, A. Liashenko, P. Piskorz, I. Komaromi, R. L. Martin, D. J. Fox, T. Keith, M. A. Al-Laham, C. Y. Peng, A. Nanayakkara, M. Challacombe, P. M. W. Gill, B. Johnson, W. Chen, M. W. Wong, C. Gonzalez, and J. A. Pople, *Gaussian 03, Revision E.01*, Gaussian Inc., Wallingford, CT (2004).
13. M. H. Jamróz, *Vibrational Energy Distribution Analysis VEDA 4*, Warsaw (2004).
14. E. Cances, B. Mennucci, and J. Tomasi, *J. Chem. Phys*., **107**, 3032 (1997).
15. *Stoe & Cie X–AREA (Version 1.18) X–RED32 (Version 1.04)*, Stoe&Cie, Darmstadt, Germany (2002).

16. G. M. Sheldrick, *SHELXS97, SHELXL97*, University of Gottingen, Germany (1997).
17. L. J. Farrugia, *J. Appl. Crystallogr*., **30**, 565 (1997).
18. E. Temel, C. Albayrak, O. Büyükgüngör, and M. Odabasogulu, *Acta Crystallogr*., **E62** o4484 (2006).
19. J. P. Jasinski, R. J. Butcher, H. S. Yathirajan, B. Narayana, and T. V. Sreevidya, *Acta Crystallogr*., **E64,** o585/o586 (2008).
20. J. N. Lisgarten, B. S. Potter, C. Bantuzeko, and R. A. Palmer, *J. Chem. Crystallogr*., **28**, No. 7, 539-543 (1998).
21. J. W. Balfour, *Spectrochim. Acta, Part A*, **39,** 795 (1983).
22. B. Lakshmaiah and G. R. Rao, *J. Raman Spectrosc*., **20,** 439 (1989).
23. B. Lakshmaiah and G. R. Rao, *Indian J. Pure Appl. Phys*., **29,** 370 (1991).
24. B. V. Reddy and G. R. Rao, *Vib. Spectrosc*., **6,** 231 (1994).
25. V. A. Babu, B. Lakshmaiah, K. S. Ramulu, and G. R. Rao, *Indian J. Pure Appl. Phys*., **25,** 58 (1987).
26. N. L. Owen and R. E. Hester, *Spectrochim. Acta, Part A*, **25,** 343 (1969).
27. G. E. Compagnaro and J. L. Wood, *J. Mol. Struct*., **6,** 117 (1970).
28. D. N. Singh and R. A. Yadav, *Asian Chem. Lett*., **2,** 65 (1998).
29. I. Yalcin, E. Sener, S. Ozden, T. Ozden, and A. Akin, *Eur. J. Med. Chem*., **25**, 705-708 (1990).
30. R. M. Silverstein, G. C. Bassler, and T. C. Morril, *Spectrometric Identification of Organic Compounds*, 5th ed., John Wiley and Sons Inc., Singapore (1991).
31. K. Fukukawa and M. Ueda, *Macromolecules*, **39**, 2100-2106 (2006).
32. C. Y. Panicker, H. T. Varghese, D. Philip, H. I. S. Nogueira, and K. Kastkova, *Spectrochim. Acta, Part A*, **67**, 1313-1320 (2007).
33. V. Shettigar, P. S. Patil, S. Naveen, S. M. Dharmaprakash, M. A. Sridhar, and J. Shashidhara Prasad, *J. Cryst. Growth*, **305**, 218 (2007).
34. Y. Qu and X. M. Sun, *Acta Crystallogr*., **E 61**, 3828 (2005).
35. L. X. Hong, L. X. Ru, and Z. X. Zhou, *Spectrochim. Acta, Part A*, **78**, 528-536 (2011).
36. M. Gussoni and C. Castiglioni, *J. Mol. Struct*., **651**, 151 (2003).
37. M. K. Rofouei, N. Sohrabi, M. Shamsipur, E. Fereyduni, S. Ayyappan, and N. Undaraganesan, *Spectrochim. Acta, Part A*, **76**, 182-190 (2010).
38. V. Bernat, N. Saffon, M. Maynadier, H. Vial, and C. Andre-Barres, *Tetrahedron*, **65,** 7372-7379 (2009).
39. S. R. Salman, S. H. Shawkat, and G. M. Al-Obaidi, *Spectrosc. Lett*., **22,** 1265 (1989).